J|A|C|S
ARTICLES
Published on Web 05/04/2006

Polymorphism of the Signaling Molecule c-di-GMP

Zhaoying Zhang, Seho Kim, Barbara L. Gaffney, and Roger A. Jones*

Contribution from the Department of Chemistry and Chemical Biology, 610 Taylor Road, Rutgers, The State University of New Jersey, Piscataway, New Jersey 08854

Received February 27, 2006; E-mail: jones@rutchem.rutgers.edu

Abstract: Using UV, CD, and NMR, we demonstrate that the important bacterial signaling molecule involved in biofilm formation, cyclic diguanosine monophosphate (c-di-GMP), exists as a mixture of five different but related structures in an equilibrium that is sensitive both to its concentration and to the metal present. At the lower concentrations used for UV and CD work (0.05−0.5 mM), Li^+, Na^+, Cs^+, and Mg^{2+} favor a bimolecular self-intercalated structure, while K^+, Rb^+, and NH_4^+ favor formation of one or more guanine quartet complexes as well. At the higher NMR concentrations (∼30 mM), the bimolecular structures associate and rearrange to a mixture of all-syn and all-anti tetramolecular and octamolecular quartet complexes. With K^+ the octamolecular complexes predominate, while with Li^+ the tetramolecular and octamolecular quartet complexes are present in approximately equal amounts, along with the bimolecular structure. We also find that both guanine amino groups in c-di-GMP are essential for formation of the quartets, because substitution of inosine for one guanosine allows formation of only the bimolecular structure. Further, two molecules of c-di-GMP tethered together are constrained in such a way that limits their ability to form these quartet complexes. The polymorphism we describe may provide different options for this signaling molecule when performing its functions in a bacterial cell, with K^+ and its own local concentration controlling the equilibrium.

Introduction

The importance of cyclic diguanosine monophosphate, c-di-GMP, **1** (Figure 1), as a ubiquitous intracellular bacterial signaling molecule responsible for regulating biofilm formation, cell differentiation, and a variety of pathogenic processes has recently been recognized.[1] Biofilms are complex, multicellular aggregations of bacteria attached to surfaces and encased in a matrix of polysaccharides.[2] Formation of such communities is an ancient adaptation that allows bacteria to survive a range of environmental challenges in a protected state. The medical, industrial, and environmental threat of biofilms for human life is profound, because they are far more resistant than free-living bacteria to antimicrobials as well as to natural host defense mechanisms.[3] Not only are antibiotics typically ineffective in treating chronic infections protected by biofilms, but low doses of aminoglycosides have recently been shown to actually induce biofilm formation in *Pseudomonas aeruginosa* and *Escherichia coli* through a mechanism controlled by c-di-GMP.[4]

Specific c-di-GMP cyclases with GGDEF domains in many different bacteria are responsible for formation of c-di-GMP from two molecules of GTP,[5,6] and a crystal structure has been determined for the cyclase from *Caulobacter crescentus*.[7] c-di-GMP levels in *P. aeruginosa*, *E. coli*, *Vibrio cholerae*,

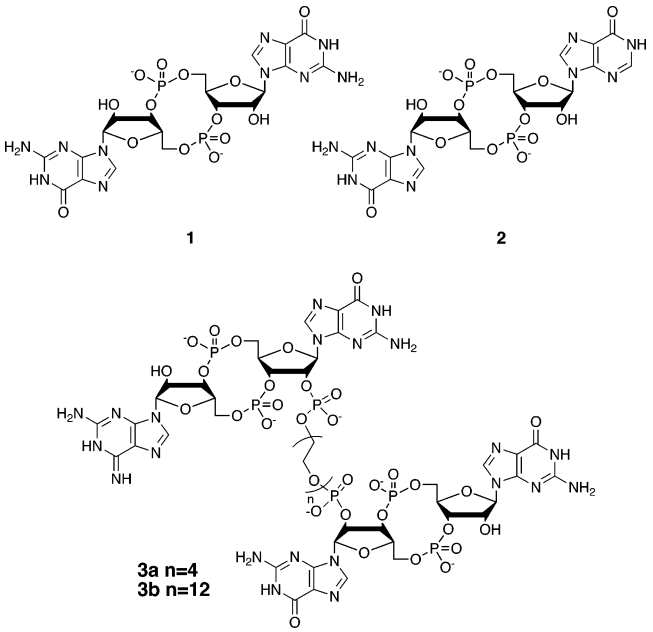

Figure 1. Structures of c-di-GMP, **1**, c-GMP−IMP, **2**, and oligoethylene-oxide tethered c-di-GMP, **3a** ($n = 4$) and **3b** ($n = 12$).

(1) Jenal, U. *Curr. Opin. Microbiol.* **2004**, *7*, 185−191. Romling, U.; Gomelsky, M.; Galperin, M. Y. *Mol. Microbiol.* **2005**, *57*, 629.
(2) Hall-Stoodley, L.; Costerton, J. W.; Stoodley, P. *Nat. Rev. Microbiol.* **2004**, *2*, 95−108.
(3) Stewart, P. S.; Costerton, J. W. *Lancet* **2001**, *358*, 135−138. Mah, T.-F. C.; O'Toole, G. A. *Trends Microbiol.* **2001**, *9*, 34−39.
(4) Hoffman, L. R.; D'Argenio, D. A.; MacCoss, M. J.; Zhang, Z.; Jones, R. A.; Miller, S. I. *Nature (London)* **2005**, *436*, 1171−1175.
(5) Paul, R.; Weiser, S.; Amiot, N. C.; Chan, C.; Schirmer, T.; Giese, B.; Jenal, U. *Genes Dev.* **2004**, *18*, 715−727.
(6) Ryjenkov, D. A.; Tarutina, M.; Moskvin, O. V.; Gomelsky, M. *J. Bacteriol.* **2005**, *187*, 1792−1798.
(7) Chan, C.; Paul, R.; Samoray, D.; Amiot, N. C.; Giese, B.; Jenal, U.; Schirmer, T. *Proc. Natl. Acad. Sci. U.S.A.* **2004**, *101*, 17084−17089.

Salmonella enterica, and *Yersinia pestis* have been shown to be inversely regulated by such cyclases along with specific phosphodiesterases associated with EAL domains.[8,9] Many bacterial proteins contain both GGDEF and EAL domains,[10] and in *C. crescentus*, a phosphodiesterase with an active EAL domain has recently been found to be regulated by the binding of GTP to its neighboring catalytically inactive GGDEF domain.[11] Thus, control of c-di-GMP concentrations in bacteria is extremely complex and may also involve gradients as well as spatial localization.[12]

As an intracellular signaling molecule, c-di-GMP is known to regulate cell mobility,[5] production of adhesive components,[8,13] and other features of multicellular behavior in response to environmental cues.[12] It also plays an important role in the pathogenic virulence of *Salmonella* in mice[14] and virulence gene expression in *V. cholerae*.[15] A group of extracellular signaling molecules termed autoinducers also regulate biofilm formation and virulence in bacteria through a process known as quorum sensing.[16] Examples include acyl homoserine lactones,[17] modified oligopeptides,[18] modified quinolones,[19] and a possible universal autoinducer, AI-2.[20] The integration of these extracellular signals with the c-di-GMP pathways is only now being explored.[21] To date, the molecular mechanisms for these complex pathways remain unknown and represent a major challenge. Although several crystal structures for c-di-GMP published some time ago revealed a self-intercalated arrangement of two molecules,[22,23] structures in solution have not been determined. Understanding the structure and behavior of c-di-GMP in solution would provide valuable insight into how it might interact with the multitude of other molecules involved in its pathways.

We recently reported a new method for the efficient synthesis of c-di-GMP, **1**, as well as UV, CD, and 1D NMR results that demonstrated a monovalent metal ion-dependent polymorphism.[24] We found evidence for a stacked structure with Li^+ and Na^+, and the suggestion of a quartet structure with K^+. We now describe UV and CD data for additional metals that further define these forms, and we have initiated more detailed structural studies using 2D NMR. We have also synthesized a mixed dimer containing guanosine and inosine, c-GMP−IMP, **2** (Figure 1), and found that the elimination of one amino group precluded quartet formation. Further, in an effort to evaluate the consequences of molecular constraints on the behavior of **1**, we have connected two units together with a flexible oligoethylene oxide tether of two different lengths, **3a** where $n = 4$ and **3b** where $n = 12$ (Figure 1). This constraint also has a significant effect on the equilibrium, shifting it substantially to the self-intercalated structure. The new data support the existence of five distinct but related complexes for **1** that exist in an equilibrium that is sensitive to both concentration and the metal present.

Experimental Procedures

Synthesis. The detailed procedures for synthesis of c-GMP−IMP, **2**, and the tethered c-di-GMP, **3a** and **3b**, are described in the Supporting Information.

UV. UV melting curves were obtained on an Aviv 14 UV spectrophotometer using 1, 2, 5, and 10 mm path length cells. After preparation in the appropriate buffer, samples were degassed, heated to 80 °C, allowed to cool slowly to room temperature, and then placed in a refrigerator for at least 15 h. UV absorbance spectra were obtained using samples in the 1 mm cells.

CD. CD spectra were obtained on an Aviv model 60DS CD spectrometer using a 1 mm cell. The samples were prepared as described for UV. For time-dependent CD experiments, data at a given wavelength were acquired immediately after the temperature was changed. The effective temperature change rate of the instrument was 10 °C/min.

1D NMR. The ^{31}P NMR spectra were acquired on a Varian Mercury 300 MHz spectrometer and referenced to 10% phosphoric acid in D_2O; the ^1H NMR spectra were acquired on a Varian Unity 400 MHz spectrometer.

2D NMR. 2D NOESY (nuclear Overhauser effect spectroscopy), HMBC (heteronuclear multiple bond correlation), and HMQC (heteronuclear multiple quantum coherence) spectra were acquired at 25 °C on a Varian Inova 500 MHz spectrometer. NOESY data were collected by 4096 (t2) times 512 (t1) complex data points with spectral widths of 8000 Hz in both dimensions and transformed to spectra with 2048 (D1) times 1024 (D2) real data points. The mixing time for NOESY spectra was 150 ms, the number of scans per each t1 increment was 16, and the relaxation delay for each scan was 2 s. Natural abundance $^1H-^{13}C$ HMQC and HMBC were acquired by 2048 (t2) times 256 (t1) complex points with spectral widths of 8000 Hz (t2) and 18000 Hz (t1) and transformed to spectra with 2048 (D1) times 512 (D2) real points. The DEPT transfer delay in HMQC was chosen as $0.5/^1J_{HC}$ with $^1J_{HC} = 150$ Hz, and the transfer delay in HMBC was chosen as $0.5/^{2,3}J_{HC}$ ($^{2,3}J_{HC} = 12$ Hz), which is close to multiples of $0.5/^1J_{HC}$ to suppress HMQC peaks. The HMBC pulse sequence and data collection mode (phase sensitive mode) were the same as HMQC with decoupling during ^1H data acquisition. The number of scans was 32 for HMQC and 256 for HMBC, and the relaxation delay for each scan was 1 s. All 2D NMR spectra used 1 s ^1H presaturation during the relaxation delay to suppress water.

(8) Simm, R.; Morr, M.; Kader, A.; Nimtz, M.; Romling, U. *Mol. Microbiol.* **2004**, *53*, 1123−1134. Tischler, A. D.; Camilli, A. *Mol. Microbiol.* **2004**, *53*, 857−869.
(9) Bobrov, A. G.; Kirillina, O.; Perry, R. D. *FEMS Microbiol. Lett.* **2005**, *247*, 123−130.
(10) Galperin, M. Y.; Nikolskaya, A. N.; Koonin, E. V. *FEMS Microbiol. Lett.* **2001**, *203*, 11−21.
(11) Christen, M.; Christen, B.; Folcher, M.; Schauerte, A.; Jenal, U. *J. Biol. Chem.* **2005**, *280*, 30829−30837.
(12) Romling, U. *Cell. Mol. Life Sci.* **2005**, *62*, 1234−1246.
(13) Ross, P.; Weinhouse, H.; Aloni, Y.; Michaeli, D.; Weinberger-Ohana, P.; Mayer, R.; Braun, S.; de Vroom, E.; van der Marel, G. A.; van Boom, J. H.; Benziman, M. *Nature* **1987**, *325*, 279−281.
(14) Hisert, K. B.; MacCoss, M.; Shiloh, M. U.; Darwin, K. H.; Singh, S.; Jones, R. A.; Ehrt, S.; Zhang, Z.; Gaffney, B. L.; Gandotra, S.; Holden, D.; Murray, D.; Nathan, C. *Mol. Microbiol.* **2005**, *56*, 1234−1245.
(15) Tischler, A. D.; Camilli, A. *Infect. Immun.* **2005**, *73*, 5873−5882.
(16) Waters, C. M.; Bassler, B. L. *Annu. Rev. Cell Dev. Biol.* **2005**, *21*, 319−346.
(17) Fuqua, C.; Parsek, M. R.; Greenberg, E. P. *Annu. Rev. Gen.* **2001**, *35*, 439−468.
(18) Kleerebezem, M.; Quadri, L. E.; Kuipers, O. P.; de Vos, W. M. *Mol. Microbiol.* **1997**, *24*, 895−904.
(19) Pesci, E. C.; Milbank, J. B. J.; Pearson, J. P.; McKnight, S.; Kende, A. S.; Greenberg, E. P.; Iglewski, B. H. *Proc. Natl. Acad. Sci. U.S.A.* **1999**, *96*, 11229−11234. Deziel, E.; Lepine, F.; Milot, S.; He, J.; Mindrinos, M. N.; Tompkins, R. G.; Rahme, L. G. *Proc. Natl. Acad. Sci. U.S.A.* **2004**, *101*, 1339−1344.
(20) Chen, X.; Schauder, S.; Potier, N.; Van Dorsselaer, A.; Pelczer, I.; Bassler, B. L.; Hughson, F. M. *Nature (London)* **2002**, *415*, 545−549. McKenzie, K. M.; Meijler, M. M.; Lowery, C. A.; Boldt, G. E.; Janda, K. D. *Chem. Commun.* **2005**, 4863−4865.
(21) Camilli, A.; Bassler, B. L. *Science* **2006**, *311*, 1113−1116.
(22) Egli, M.; Gessner, R. V.; Williams, L. D.; Quigley, G. J.; van der Marel, G. A.; van Boom, J. A.; Rich, A.; Frederick, C. A. *Proc. Natl. Acad. Sci. U.S.A.* **1990**, *87*, 3235−3239.
(23) Liaw, Y.-C.; Gao, Y.-G.; Robinson, H.; Sheldrick, G. M.; Sliedregt, L. A. J. M.; van der Marel, G. A.; A., v. B. J.; Wang, A. H.-J. *FEBS Lett.* **1990**, *264*, 223−227. Guan, Y.; Gao, Y.-G.; Liaw, Y.-C.; Robinson, H.; Wang, A. H.-J. *J. Biomol. Struct. Dyn.* **1993**, *11*, 253−276.
(24) Zhang, Z.; Gaffney, B. L.; Jones, R. A. *J. Am. Chem. Soc.* **2004**, *126*, 16700−16701.

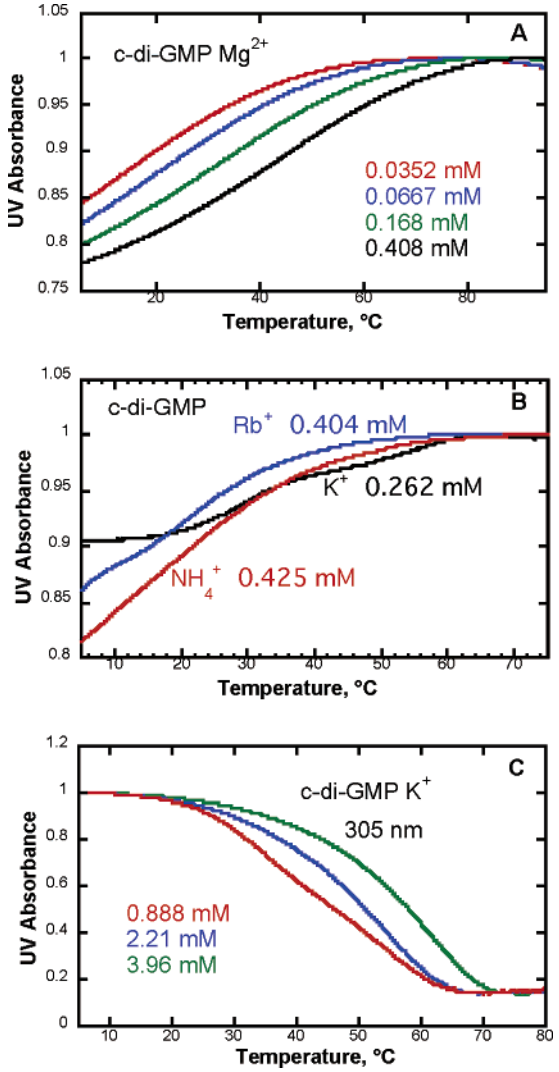

Figure 2. Normalized UV melting profiles (A) at 250 nm of four different concentrations of the Mg^{2+} form of **1** in 10 mM $Mg(OAc)_2$ with 0.1 M $MgCl_2$, pH 7.0, (B) at 250 nm of the K^+ (black), Rb^+ (blue), and NH_4^+ (red) forms of **1** in 10 mM potassium phosphate with 0.1 M KCl, 10 mM rubidium phosphate with 0.1 M RbCl, and 10 mM ammonium phosphate with 0.1 M NH_4Cl, respectively, all pH 7.0, and (C) at 305 nm of three different concentrations of the K^+ form of **1** in 10 mM potassium phosphate with 0.1 M KCl.

Results

1. c-di-GMP. UV Melts. UV melting profiles at 250 nm for four different concentrations of **1** with Mg^{2+} (Figure 2A) show single conformational transitions similar to those with Li^+ and Na^+,[24] but reflect a more thermally stable structure. First derivative curves for the most concentrated sample with each metal (Supporting Information) show one clear maximum, with T_{max} values of 8 °C for Na^+, 10 °C for Li^+, and 45 °C for Mg^{2+}. The concentration dependence of the transitions with these metals indicates that the structured forms have a molecularity of at least 2.[25] Further, the significant hypochromicity of the UV curves indicates that stacking of the guanines plays an important role in the structure.

The UV melting profile at 250 nm for the Rb^+ form of **1** (Figure 2B, blue) shows two broad conformational transitions, somewhat similar to those of the K^+ form[24] (included in Figure 2B, black), but with lower stabilities. T_{max} values from first derivative curves are 30 °C/54 °C for K^+ and <5 °C/20 °C for Rb^+. Although the UV melting profile for the NH_4^+ form appears to show a single conformational transition (Figure 2B, red), its first derivative curve shows two broad overlapping maxima, with T_{max} values of 10 °C/20 °C.

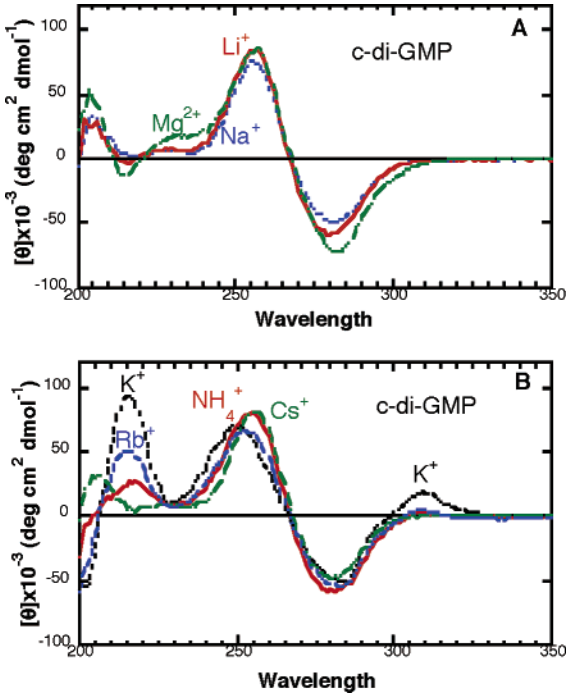

Figure 3. CD spectra of **1** at 5 °C in 0.1 cm cells of (A) 0.384 mM Li^+ form (red), 0.395 mM Na^+ form (blue), and 0.437 mM Mg^{2+} form (green) in 10 mM LiOAc with 0.1 M LiCl, 10 mM sodium phosphate with 0.1 M NaCl, and 10 mM $Mg(OAc)_2$ with 0.1 M $MgCl_2$, respectively, all at pH 7.0, and (B) 0.409 mM K^+ form (black), 0.383 mM Rb^+ form (blue), 0.382 mM Cs^+ form (green), and 0.378 mM NH_4^+ form (red) in 10 mM potassium phosphate with 0.1 M KCl, 10 mM RbOAc with 0.1 M RbCl, 10 mM CsOAc with 0.1 M CsCl, and 10 mM NH_4OAc with 0.1 M NH_4Cl, respectively, all at pH 7.0.

The UV spectrum of the K^+ form of **1** displays a distinct shoulder between 295 and 305 nm that is not present in the Li^+, Na^+, or Mg^{2+} forms, and is weak in the Rb^+ and NH_4^+ forms (Supporting Information). Because similar shoulders were found to be characteristic of intramolecular guanine quartet structures formed by a series of oligodeoxynucleotides,[26] we now report UV melting experiments at 305 nm for a series of three K^+ samples with different concentrations (Figure 2C). As seen with the quartet-forming oligonucleotides,[26] the profiles at 305 nm display hyperchromic changes rather than the typical hypochromic changes seen at 250 nm. Together, the UV results support the presence of one or more additional structures for **1** with K^+ and Rb^+ that contain guanine quartets. Further, because intramolecular guanine quartet oligonucleotides that exhibit hyperchromic behavior all contain some guanines with syn conformations,[27] by extension, at least one of the quartet structures of **1** in K^+ and Rb^+ may also contain some syn guanines.

CD Spectra. A CD spectrum of the Mg^{2+} form of **1** (Figure 3A, green) closely resembles those of Li^+ (red)[24] and Na^+ (blue).[24] Upon heating to 75 °C, the bands all quickly

(25) Marky, L. A.; Breslauer, K. J. *Biopolymers* **1987**, *26*, 1601−1620.

(26) Mergny, J.-L.; Phan, A.-T.; Lacroix, L. *FEBS Lett.* **1998**, *435*, 74−78.
(27) Keniry, M. A. *Biopolymers* **2001**, *56*, 123−146.

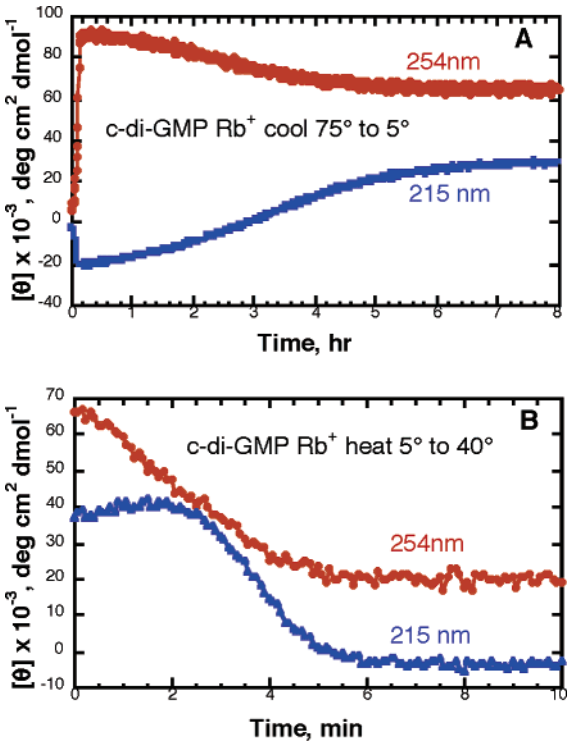

Figure 4. Plots of molar ellipticity at a given wavelength as a function of time after (A) cooling or (B) heating preequilibrated samples of the Rb^+ form of **1** in a 0.1 cm cell.

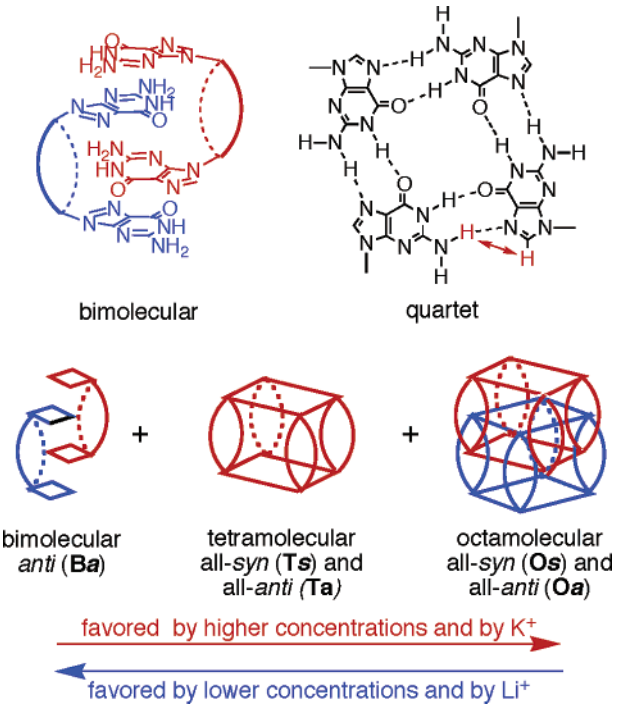

Figure 5. Cartoons of proposed structures of **1**.

diminish to small residual values (not shown). The positive band at 257 nm and the negative band at 281 nm form a pattern that is inverted relative to right-handed DNA and RNA, but is similar to CD spectra of cyclic dithymidine monophosphate,[28] 5′-GMP and 3′-GMP in 0.1 M K^+,[29] left-handed 5′-5′ GpG,[29] left-handed Z DNA,[30] and diadenosine and diguanosine 5′,5‴-oligophosphates.[31] For the Li^+, Na^+, and Mg^{2+} forms of **1**, the pattern for the 257 and 281 nm bands is consistent with the possibility of a left-handed alignment of the guanine transition moments.

The CD spectrum that we previously reported for the K^+ form of **1** displays additional bands at 215 nm (strong) and 309 nm (weak)[24] (Figure 3B, black). Further, its central positive band appears at 252 nm rather than 257 nm. We now report CD spectra for Rb^+ (blue), Cs^+ (green), and NH_4^+ (red) forms (Figure 3B). The presence of a similar 215 nm band for the Rb^+ form (although only one-half the intensity), but none for the Cs^+ form, demonstrates the same dependence on ion size shown by guanine quartets.[27,32] The Rb^+ form, but not the Cs^+ form, also displays a shift to lower wavelength for the central positive band, although only about one-half as much as for the K^+ form. The NH_4^+ form shows a weak 215 nm band and a small shift of its central band. Positive CD bands near 300 nm have been observed for oligodeoxynucleotides with intramolecular quartet structures that have a mixture of syn and anti orientations, while those with intermolecular quartets that are all anti do not have this 300 nm band.[27,33]

We have previously reported the slow appearance and disappearance of the 215 and 309 nm bands for the K^+ form of **1** (∼20 h).[24] We now report similar behavior for the Rb^+ form, where nearly 8 h is required for the full appearance of the 215 nm band upon cooling from 75 to 5 °C (Figure 4A, blue). Further, a similar cooling curve for the 254 nm band (red) displays a fast increase over minutes to a maximum value, followed by a slow decrease to a somewhat smaller value. This slow decrease of the 254 nm band correlates with the slow increase of the 215 nm band and reflects the shifting of the central positive band that presumably occurs upon quartet formation. Our previously reported data for the K^+ form at 250 nm upon cooling[24] also show a fast increase followed by a similar slow decrease that is less pronounced than with Rb^+. These results support the initial formation of a bimolecular stacked structure in K^+ and Rb^+, which then undergoes a slow association and rearrangement to one or more quartet structures.

We had already shown the slow loss of the 215 and 250 nm bands upon heating the K^+ form from 5 to 40 °C (∼20 h), consistent with both bands being associated with the quartet structure.[24] Heating the Rb^+ form from 5 to 40 °C also shows a slow loss of the 215 and 254 nm bands (Figure 4B), but over only about 10 min, consistent with the lower thermal stability of the Rb^+ quartet structure.

NMR Spectra. We previously reported 1D ^1H and ^{31}P NMR spectra for the Li^+, Na^+, and K^+ forms of ∼35 mM samples of **1** in 0.1 M LiCl, NaCl, or KCl, respectively, at pH 7.[24] The data for the K^+ form were consistent with two different types of quartet structures that were both stable even at 55 °C: one type (∼50%) displayed two guanine H8 resonances and two upfield ^{31}P resonances, and another type (∼44%) displayed only

(28) Cantor, C. R.; Fairclough, R. H.; Newmark, R. A. *Biochemistry* **1969**, *8*, 3610−3617.
(29) Chantot, J.-F.; Haertle, T.; Guschlbauer, W. *Biochemie* **1974**, *56*, 501−507.
(30) Pohl, F. M.; Jovin, T. M. *J. Mol. Biol.* **1972**, *67*, 375−396.
(31) Scott, J. F.; Zamecnik, P. C. *Proc. Natl. Acad. Sci. U.S.A.* **1969**, *64*, 1308−1314. Holler, E.; Holmquist, B.; Vallee, B. L.; Taneja, K.; Zamecnik, P. *Biochemistry* **1983**, *22*, 4924−4933.
(32) Hardin, C. C.; Perry, A. G.; White, K. *Biopolymers* **2001**, *56*, 147−194. Davis, J. T. *Angew. Chem., Int. Ed.* **2004**, *43*, 668−698.
(33) Jin, R.; Gaffney, B. L.; Wang, C.; Jones, R. A.; Breslauer, K. J. *Proc. Natl. Acad. Sci. U.S.A.* **1992**, *89*, 8832−8836.

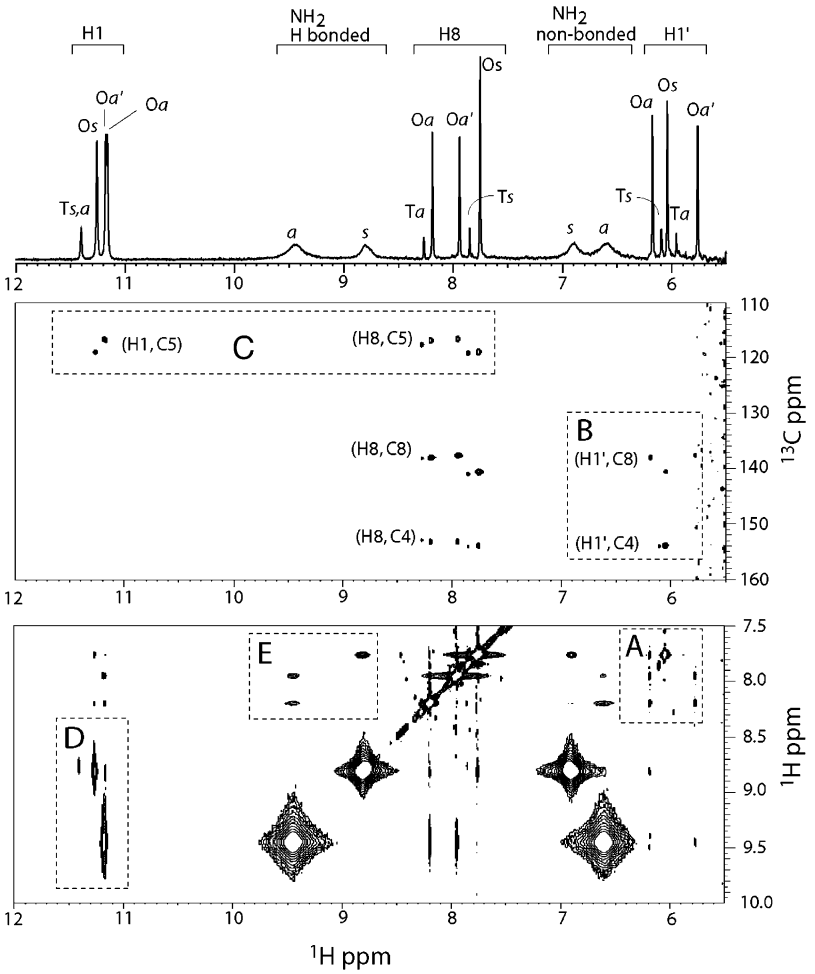

Figure 6. NMR spectra of a 37 mM sample of the K^+ form of **1** in 0.1 M KCl in 90/10 H_2O/D_2O at 25 °C, with its 1D ^1H spectrum at the top, a portion of its superimposed $^1H-^{13}C$ HMBC/HMQC spectrum at the center, and a portion of its $^1H-^1H$ NOESY spectrum at the bottom. Regions of interest are labeled to correspond with the text.

one H8 resonance and only one downfield ^{31}P resonance. Two additional minor (~2% and 4%) H8 and ^{31}P resonances were also present. ^{31}P NMR spectra at 5 °C for the Li^+ and Na^+ forms of **1** also displayed upfield and downfield resonances, but in more complex patterns.[24] These signals had significantly diminished at 55 °C, leaving a prominent central resonance near −1.0 ppm. ^1H NMR spectra at 5 °C for the Li^+ form showed six guanine H8 resonances. These results are consistent with the presence of a group of structures having lower stabilities than those of the K^+ form. Despite their different stabilities, the Li^+, Na^+, and K^+ forms in 90% H_2O all displayed ^1H resonances near 11 ppm consistent with hydrogen-bonded guanine H1s, as well as broad resonances near 9 and 6.5 ppm consistent with hydrogen-bonded and non-hydrogen-bonded guanine amino protons, respectively.[34] As described more fully in the Discussion, these previous 1D NMR results and new 2D NMR data introduced below for both the K^+ and the Li^+ forms of **1** support the presence in varying amounts of five different but related structures shown in the cartoons at the bottom of Figure 5: one bimolecular self-intercalated structure (shown in more detail at the top left of Figure 5), two tetramolecular and two octamolecular structures, all of which contain guanine quartets (shown at the top right of Figure 5, with the H8 to H-bonded amino NOE highlighted in red). The 2D NMR data described below demonstrate that the larger complexes exist in both all-syn and all-anti conformations.

The 1D spectrum of a 37 mM sample of the K^+ form of **1** in KCl at pH 7 at 25 °C is shown at the top of Figure 6, with a portion of its superimposed $^1H-^{13}C$ HMBC/HMQC spectrum at the center, and a portion of its $^1H-^1H$ NOESY spectrum at the bottom. Region A in the NOESY spectrum shows a set of H8 to H1′ cross-peaks. The three major H8 resonances show cross-peaks to H1′ resonances, of which one is significantly stronger than the other two. The different NOE intensities are consistent with a syn guanosine conformation for the stronger NOE and anti conformations for the weaker NOEs.[35] The H8 resonances at 7.75, 8.20, and 7.95 ppm, and the H1′ resonances at 6.05, 6.19, and 5.77 ppm, are therefore labeled O*s*, O*a*, and O*a*′ for octamolecular/syn and anti, respectively. There are no cross-peaks between the syn and anti resonances, while cross-peaks are observed between the two anti resonances. Of the two minor H8 resonances, one shows a stronger cross-peak to the H1′ region than the other, again indicating syn and anti conformations. The H8 resonances at 7.85 and 8.26 ppm and the H1′ resonances at 6.12 and 5.96 ppm are therefore labeled

(34) Wang, Y.; Patel, D. J. *Biochemistry* **1992**, *31*, 8112−8119. Smith, F. W.; Feigon, J. *Biochemistry* **1993**, *32*, 8682−8692.

(35) Wang, Y.; de los Santos, C.; Gao, X.; Greene, K.; Live, D.; Patel, D. J. *J. Mol. Biol.* **1991**, *222*, 819−832. Smith, F. W.; Feigon, J. *Nature (London)* **1992**, *356*, 164−1168. Wang, K. Y.; McCurdy, S.; Shea, R. G.; Swaminathan, S.; Bolton, P. H. *Biochemistry* **1993**, *32*, 1899−1904.

T*s* and T*a*, for tetramolecular/syn and anti, respectively. These NOESY cross-peaks had the same positive sign as the auto-peaks due to negative NOE enhancements and built up quite fast at a mixing time of 150 ms, which indicates that the molecular species giving rise to them are in the slow tumbling regime.[36] Because neither the monomeric (MW = 689) nor the dimeric (MW = 1378) forms of **1** in water are large enough to generate strong negative NOE enhancements, our data suggest that the four species present in this sample with K^+ are larger than the bimolecular form.

Region B in the HMBC/HMQC confirms the assignments, because the H1′ resonances labeled O*s* and T*s* show stronger cross-peaks to their C4 than to their C8 resonances, while the H1′ resonances labeled O*a* and O*a*′ do not show cross-peaks to their C4 but do to their C8 resonances. Such differences have been shown to support a syn assignment for the former and an anti assignment for the latter.[37]

The HMBC/HMQC spectrum also allows assignment of the amido H1 resonances, as shown in Region C. The large downfield H1 resonance at 11.27 ppm (O*s*) correlates only with the syn H8 resonance O*s*, while the pair of large upfield H1 resonances at 11.18 ppm (O*a* and O*a*′) both correlate only with the two anti H8 resonances, O*a* and O*a*′. From Region D in the NOESY spectrum, the broad hydrogen-bonded amino resonances can then be assigned in terms of syn and anti. The syn H1 resonance O*s* correlates only with the more upfield hydrogen-bonded amino resonance at 8.81 ppm (labeled *s*), and the anti H1 resonances O*a* and O*a*′ correlate with the more downfield hydrogen-bonded amino resonance at 9.45 ppm (labeled *a*). The minor downfield H1 resonance at 11.42 ppm, labeled T*s*,*a* because it presumably represents these two overlapping resonances, shows a cross-peak to the region of the syn amino resonance at 8.81 ppm.

Because in a given quartet each hydrogen-bonded amino is close to the H8 of its neighbor (Figure 5), the pattern of their NOE cross-peaks can define the arrangement of syn and anti conformations within each quartet.[38,39] Region E in the NOESY spectrum shows that the broad anti hydrogen-bonded amino region (*a*) has cross-peaks only to the two anti H8 resonances O*a* and O*a*′, and the broad syn hydrogen-bonded amino region (*s*) has a cross-peak only to the single syn H8 resonance O*s*. Thus, we conclude that with K^+, c-di-GMP exists primarily as two major different quartet-containing species, with the O*a*/O*a*′ structure being all-anti and the O*s* quartet structure being all-syn. The different intensities of the O*s* and O*a* resonances do not support the presence of a mixed species with one anti quartet and one syn quartet. All-anti quartets are well known in parallel guanine-containing oligodeoxynucleotides,[27,32] and all-syn quartets have been found in lipophilic guanine quartet assemblies.[38,40]

A 1D NMR spectrum of a 33 mM sample of the Li^+ form of **1** in 0.1 M LiCl at pH 7 at 25 °C is shown at the top of Figure 7, with a portion of its superimposed $^1H-^{13}C$ HMBC/HMQC spectrum at the center and a portion of its $^1H-^1H$ NOESY spectrum at the bottom. Although the relative intensities of the resonances are quite different from those of the K^+ form, the 2D spectra are strikingly similar. Region A in the NOESY spectrum shows significant cross-peaks from the two most upfield H8 resonances (T*s* at 7.83 and O*s* at 7.74 ppm) to H1′ resonances, but weak cross-peaks from the three more downfield H8 resonances (T*a* at 8.25, O*a* at 8.19, and O*a*′ at 7.95 ppm) to H1′ resonances. These NOE cross-peaks were also positive with strongly negative NOE enhancements, similar to those with K^+. However, no cross-peak is seen for the sixth resonance at 7.90 ppm, labeled B*a* for bimolecular/anti. These results indicate the presence of the same syn and anti structures as with the K^+ form, although in more similar amounts, and with one additional structure. The HMBC/HMQC spectrum again confirms these assignments, as shown in Region B. Further, for the sixth H8 resonance at 7.90 ppm (B*a*), a cross-peak is seen between its corresponding H1′ resonance at 5.84 ppm to its C8, but not to its C4 resonance, indicating this additional structure has an anti conformation.

Region C of the HMBC/HMQC spectrum again allows assignment of the amido H1 resonances. The most downfield H1 resonance at 11.38 ppm (T*a*) correlates only with the H8 resonance T*a* at 8.25 ppm; the center two H1 resonances at 11.36 and 11.23 ppm (T*s* and O*s*) correlate with H8 resonances T*s* at 7.83 ppm and O*s* at 7.74 ppm; and the upfield H1 resonance at 11.14 ppm (O*a*,*a*′) correlates with H8 resonances O*a* at 8.19 ppm and O*a*′ at 7.95 ppm. From Region D in the NOESY spectrum, the hydrogen-bonded amino resonances again can be assigned in terms of syn and anti. The anti H1 resonance

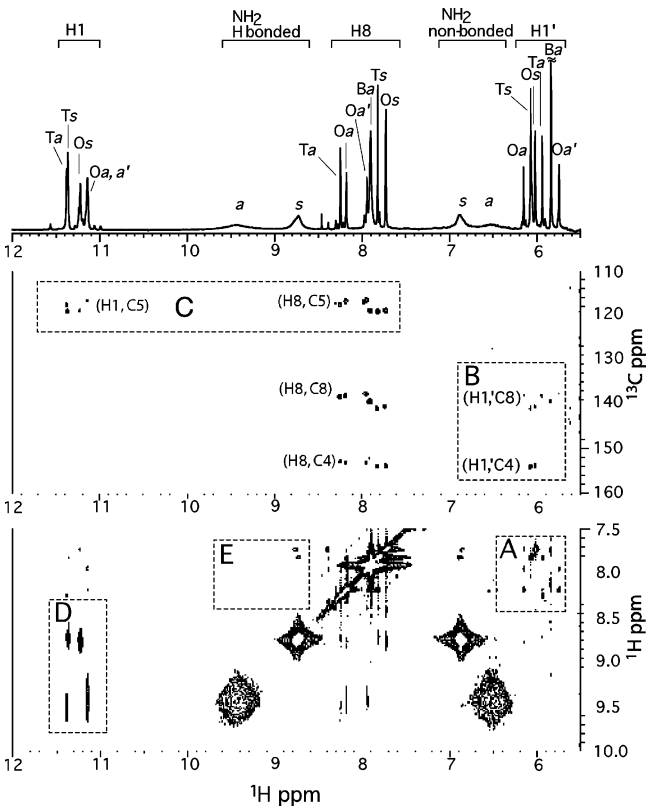

Figure 7. NMR spectra of a 33 mM sample of the Li^+ form of **1** in 0.1 M LiCl in 90/10 H_2O/D_2O at pH 7 at 25 °C, with its ^1H 1D spectrum at the top, a portion of its superimposed $^1H-^{13}C$ HMBC/HMQC spectrum at the center, and a portion of its $^1H-^1H$ NOESY spectrum at the bottom. Regions of interest are labeled to correspond with the text.

(36) Cavanagh, J.; Fairbrother, W. J.; Palmer, A. G., III; Skelta, N. J. *Protein NMR Spectroscopy*, Academic Press: San Diego, CA, 1996; pp 289−290.
(37) Zhu, G.; Live, D.; Bax, A. *J. Am. Chem. Soc.* **1994**, *116*, 8370−8371.
(38) Marlow, A. L.; Mezzina, E.; Spada, G. P.; Masiero, S.; Davis, J. T.; Gottarelli, G. *J. Org. Chem.* **1999**, *64*, 5116−5123.
(39) Phan, A. T.; Patel, D. J. *J. Am. Chem. Soc.* **2003**, *125*, 15021−15027.
(40) Forman, S. L.; Fettinger, J. C.; Pieraccini, S.; Gottarelli, G.; Davis, J. T. *J. Am. Chem. Soc.* **2000**, *122*, 4060−4067.

T*a* correlates with the more downfield hydrogen-bonded amino region at 9.42 ppm (*a*); the syn H1 resonance T*s* correlates with the more upfield hydrogen-bonded amino region at 8.85 ppm (*s*); the syn resonance O*s* correlates with the *s* amino region; and the anti H1 resonance O*a* correlates with the *a* amino region. Region E in the NOESY spectrum shows two cross-peaks for the broad syn hydrogen-bonded amino region (*s*), one to the H8 resonance O*s* and one to the H8 resonance T*s*. The anti hydrogen-bonded amino (*a*) is apparently too weak to show analogous cross-peaks. These data are again consistent with an O*a*/O*a*′ quartet structure that is all-anti and an O*s* quartet structure that is all-syn.

The NOESY data described above suggest that the two major and the two minor species with K^+ all have molecular weights larger than the bimolecular form. To obtain additional information, NMR diffusion experiments were performed. The data (Supporting Information) show that, with K^+, the translational diffusion rates of the two major forms, O*a* and O*s*, are similar to each other, but smaller than those of the two minor forms, T*a* and T*s*, which are also similar to each other. These results demonstrate that O*a* and O*s* have a higher molecular weight than T*a* and T*s*. The measured diffusion rates of these four species agree well with the published range of DNA diffusion rates.[41] Diffusion data for the Li^+ form show a similar pattern in that the rates for T*a* and T*s* are larger than those for O*a* and O*s*. The rate for the fifth form, B*a*, was considerably larger than any of the other species, demonstrating a smaller molecular weight that is consistent with a bimolecular complex. The absolute values of the rates for the analogous species in the two samples are slightly different, perhaps because the samples are not identical.

These new UV, CD, and NMR results together present a compelling case for the presence of a mixture of five different structures that **1** can adopt, whose ratio is both metal and concentration-dependent. As discussed more fully below, a bimolecular structure (B*a*) is dominant with Li^+, Na^+, Cs^+, and Mg^{2+} at dilute concentrations of **1**, but is accompanied by one or more quartet structures with K^+ and Rb^+. At the higher NMR concentrations, with K^+ the bimolecular structures associate and rearrange primarily to two stable higher molecular weight quartet structures, one all-syn (O*s*) and one all-anti (O*a*), with two minor lower molecular weight quartet structures also present, T*s* and T*a*. With Li^+, the bimolecular structure (B*a*) predominates, but both quartet structures (O*a*, O*s*, T*a*, and T*s*) are also present.

2. c-GMP−IMP, 2. We have now synthesized a mixed cyclic dimer containing one guanosine and one inosine, **2** (Figure 1), by a method similar to what we previously reported for **1**.[24] In brief, an intermolecular coupling using phosphoramidite chemistry was followed by an H-phosphonate cyclization, with the H-phosphonate group also serving as a 3′ protecting group during the initial coupling. The detailed procedures are described in the Supporting Information. We describe below UV, CD, and NMR spectra for this molecule that has one fewer amino group than **1**.

UV Melts. UV melting profiles (Figure 8A) at 250 nm for different concentrations of **2** with both Li^+ and K^+ show single concentration-dependent conformational transitions that are identical for the two cations and reflect a more stable structure

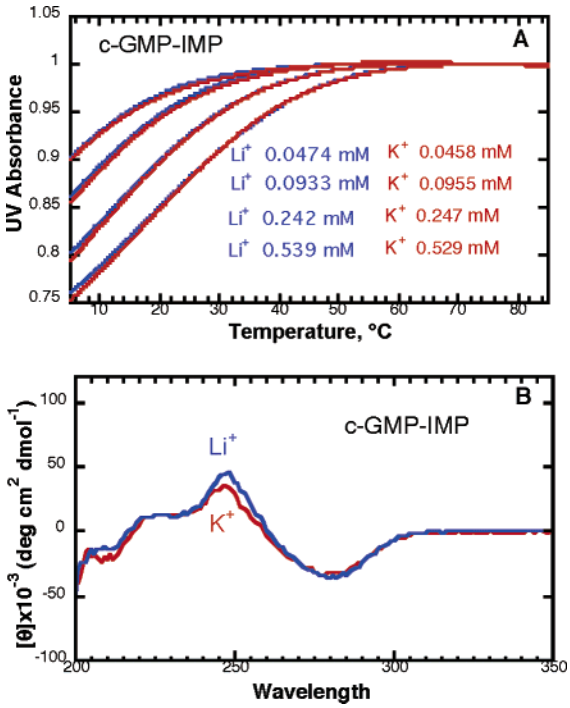

Figure 8. (A) Normalized UV melting profiles at 250 nm of four different concentrations of Li^+ (blue) and K^+ (red) forms of **2** in 10 mM LiOAc with 0.1 M LiCl, and 10 mM potassium phosphate with 0.1 M KCl, respectively, both pH 7.0, and (B) CD spectra at 5 °C in 0.1 cm cells of 0.537 mM Li^+ form (blue) and 0.544 mM K^+ form (red) of **2** in 10 mM LiOAc with 0.1 M LiCl, and 10 mM potassium phosphate with 0.1 M KCl, respectively, both at pH 7.0.

than the Li^+ form of **1**. The T_{max} values of the most concentrated samples of both forms of **2** were found to be 18 °C, while the T_{max} value for the Li^+ form of **1** was only 10 °C. These results suggest that loss of one of the guanine amino groups prevents formation of quartet structures in K^+, but allows a bimolecular stacked structure.

CD Spectra. CD spectra (Figure 8B) for the Li^+ and K^+ forms of **2** are nearly identical and display much lower intensities than the Li^+ form of **1**, perhaps due to the different absorption properties of inosine. The lack of any bands near 215 and 305 nm supports the absence of quartet structures.

NMR Spectra. The 1D NMR spectra for 61 mM samples of the Li^+ and K^+ forms of **2** at 5, 30, and 55 °C (Supporting Information) are much simpler than those for **1**. Both ^{31}P NMR spectra of **2** at 5 °C show only two resonances near −1.5 ppm, one for each of the different phosphates in the molecule. Neither of the ^1H NMR spectra in 90% H_2O at 5 °C shows H1 resonances near 11 ppm or amino resonances near 9 and 6.5 ppm, demonstrating the exchange of these protons with solvent. Further, single sharp resonances are present for the guanine H8 and the inosine H8 and H2. As seen in Figure 9, the $^1H-^1H$ NOESY spectrum for **2** with K^+ does not show cross-peaks between the H8 and H1′ resonances, but the $^1H-^{13}C$ HMBC/HMQC spectrum does show cross-peaks between the two H1′ resonances and their C8 resonances, but not their C4 resonances, indicating anti conformations. Thus, absence of one amino group precludes quartet formation but allows a bimolecular anti stacked structure in which the amido and amino protons exchange readily with solvent.

3. Oligoethyleneoxide Tethered c-di-GMP, 3a and 3b. We have also linked two molecules of **1** together with flexible

(41) Lapham, J.; Rife, J. P.; Moore, P. B.; Crothers, D. M. *J. Biomol. NMR* **1997**, *10*, 255−262.

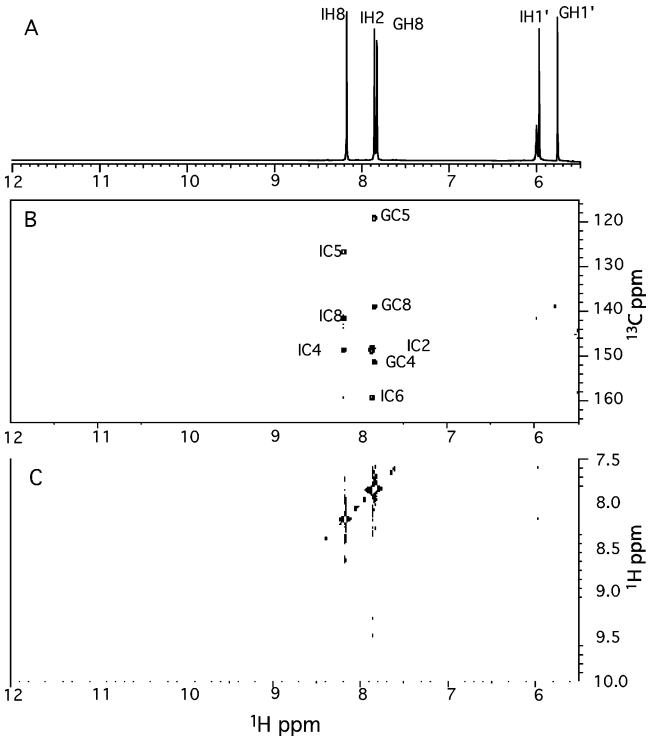

Figure 9. NMR spectra of a 60.8 mM sample of the K^+ form of **2** in 90/10 H_2O/D_2O at 25 °C, with its 1D spectrum at the top, a portion of its superimposed $^1H-^{13}C$ HMBC/HMQC spectrum at the center, and a portion of its $^1H-^1H$ NOESY NMR spectrum at the bottom.

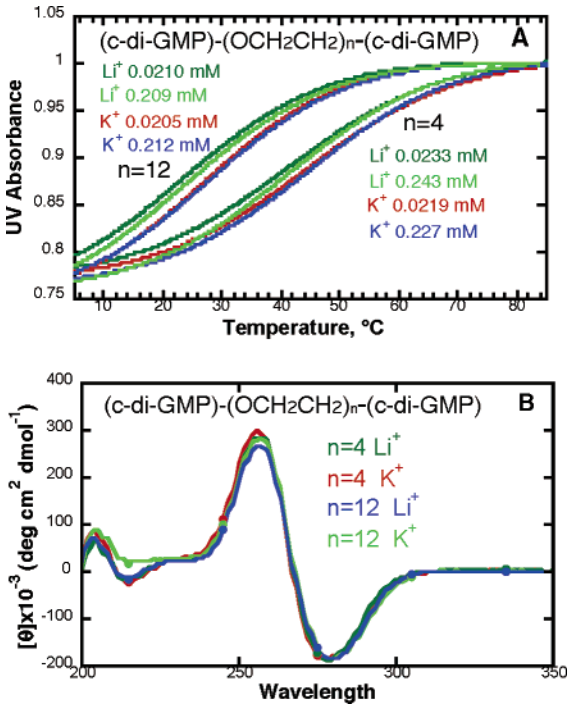

Figure 10. (A) Normalized UV melting profiles at 250 nm of two different concentrations each of the Li^+ (dark and light green) and K^+ (red and blue) forms of **3a** and **3b** in 10 mM LiOAc with 0.1 M LiCl, and 10 mM potassium phosphate with 0.1 M KCl, respectively, both pH 7.0, and (B) CD spectra at 5 °C in 0.1 cm cells of 0.227 mM Li^+ form (dark green) and 0.227 mM K^+ form (red) of **3a** in 10 mM LiOAc with 0.1 M LiCl, and 10 mM potassium phosphate with 0.1 M KCl, respectively, and 0.209 mM Li^+ form (blue) and 0.212 mM K^+ form (light green) of **3b** in 10 mM LiOAc with 0.1 M LiCl, and 10 mM potassium phosphate with 0.1 M KCl, respectively, all at pH 7.0.

oligoethyleneoxide tethers of 4 (**3a**) or 12 (**3b**) units (Figure 1), thereby constraining their interactions. Their syntheses and 1D NMR spectra are described in the Supporting Information, and their UV and CD data are presented below.

UV Melts. UV melting profiles (Figure 10A) at 250 nm for two different concentrations each of **3a** and **3b** with Li^+ and K^+ show hypochromic conformational transitions that have very little concentration dependence. Further, for both tether lengths, the K^+ forms are only slightly more stable than the Li^+ forms. The transitions are thus primarily intramolecular and cation independent. The structured forms of **3b** have T_{max} values of 24 °C with Li^+ and 26 °C with K^+, significantly lower than those of **3a**, which have T_{max} values of 42 °C with Li^+ and 44 °C with K^+. The similar hypochromicity in both metals indicates that the tethers allow intramolecular formation of related stacked structures, while the lower stabilities with the longer tether may be due to entropic factors.

CD Spectra. CD spectra (Figure 10B) for the Li^+ and K^+ forms of **3a** and **3b** are nearly identical to each other and similar to the CD spectrum of **1** with Li^+. The lack of any bands near 215 or 305 nm shows that the tether precludes formation of guanine quartets at this concentration.

NMR Spectra (Supporting Information). As with **2**, the 1D ^1H and ^{31}P NMR spectra of a 15 mM sample of the Li^+ form of **3a** are much simpler than those of **1**. The ^{31}P NMR spectrum shows only three resonances near −2.0 ppm, one for each type of phosphate in the molecule. The ^{31}P NMR spectrum of a 13 mM sample of the K^+ form also gives three dominant resonances near −2.0 ppm, but smaller clusters of signals are present upfield and downfield as well. The ^1H NMR spectrum of the Li^+ form shows no H1 signals near 11 ppm or amino signals near 9 and 6.5 ppm, signifying their exchange with solvent. Single sharp resonances are present for each of the two types of guanine H8, one of which is closer to the tether and the other farther away. The K^+ form also shows two dominant sharp H8 resonances, but a cluster of several smaller H8 resonances is also present. Further, there are several small H1 resonances near 11 ppm and amino resonances near 9 and 6.5 ppm. The UV, CD, and NMR results for **3a** with Li^+ are consistent with the presence of only a unimolecular self-intercalated structure related to the bimolecular self-intercalated structure of **1**, B*a*. With K^+, the results support the presence of a mixture with the major component being the self-intercalated structure, but with small amounts of quartet complexes also present. Because the concentration of **3a** with K^+ (26 mM in terms of guanine) is similar to that of **1** with K^+ (37 mM in guanine), we conclude that the tether makes formation of a quartet structure significantly more difficult, but allows the self-intercalated structure to readily form.

Discussion

On the basis of the UV, CD, and NMR data presented above and in our earlier report,[24] we propose that c-di-GMP can adopt five different but related structures, all participating in an equilibrium that is sensitive to both concentration of **1** and the metal present. The cartoons at the bottom of Figure 5 depict these five structures: an anti bimolecular self-intercalated complex, syn and anti versions of a tetramolecular quartet complex, and syn and anti versions of an octamolecular self-intercalated quartet complex. The UV concentration dependence

and hypochromicity, as well as the strong CD spectra, demonstrate the presence of intermolecular guanine stacking. At dilute concentrations with Li^+, Na^+, Cs^+, or Mg^{2+}, **1** forms the self-intercalated bimolecular complex that had been found in crystal structures reported for **1** in the presence of Mg^{2+} or Co^{2+},[22,23] as well as for **1** associated with its cyclase from *Caulobacter crescentus*.[7] At the higher NMR concentrations with Li^+, single H8 and ^{31}P resonances are seen from this structure. Although this complex has two different types of phosphates and guanines (inner and outer), and the amido H1s and aminos of the inner guanines may be oriented so as to form hydrogen bonds with a phosphate of its partner, our data are consistent with this self-intercalated structure being in fast exchange on the NMR time scale with an unstructured form. Thus, no amido or amino resonances are present and only single H8, H1′, and ^{31}P resonances are observed. The lack of positive NOE cross-peaks and the relatively large translational diffusion rate support the lower molecular weight of a bimolecular complex.

Our data indicate that the tethered c-di-GMP (**3a** and **3b**) as well as c-GMP−IMP (**2**) are also able to adopt this self-intercalated structure, despite the constraints of the tethers and lack of one amino, respectively. Their UV spectra show significant hypochromicity, and the CD spectra of **3a** and **3b** are nearly identical to those of **1**. The smaller intensity of the CD spectrum of **2** is most likely because of the altered absorption properties of inosine. Both the 1D and the 2D NMR data are consistent with the predominant presence of this self-intercalated structure in the Li^+ and K^+ forms of **2** and **3a**.

At low concentrations of **1** with K^+, Rb^+, and NH_4^+, our UV and CD data strongly support the presence of one or more additional structures containing guanine quartets. The UV melt of the K^+ form of **1** at 250 nm displays two transitions, and its melt at 305 nm shows characteristics of oligodeoxynucleotides containing quartets with syn conformations. The CD spectra with these metals display new bands at 215 and 309 nm that are slow to appear and diminish, consistent with a higher molecularity. At the higher NMR concentrations of the K^+ form, ^1H and ^{31}P NMR resonances distinct from those corresponding to the bimolecular structure persist at 55 °C. The ^1H NMR spectra, both 1D and 2D, are consistent with two major structures, both of which have similar and relatively high molecular weights. One has two sets of H8, H1′, and ^{31}P resonances, to which we can assign anti conformations, and the other has only one set to which we can assign the syn conformation. The NMR spectra also show two minor structures with similar and relatively smaller molecular weights that are still greater than the bimolecular form, one of which is anti and one of which is syn.

In Wang's reports on the self-intercalated crystal structure of **1** with Mg^{2+} and Co^{2+},[23] he had speculated about the possibility of its rearrangement to a cage-like complex of four molecules of **1** containing two parallel guanine quartets 7 Å apart (bottom of Figure 5, center). Although he described only an all-anti version, it might also occur in an all-syn version, and our data support the presence of these two tetramolecular quartet structures as minor components in the K^+ form of **1** at high concentrations. However, if two such all-anti or all-syn quartet complexes (a total of eight molecules of **1**) were able to self-intercalate, they should be stabilized by favorable stacking (3.5 Å apart) and additional interactions with the K^+ ions (bottom of Figure 5, right). The presence of inner and outer guanosines would account for the two sets of NMR resonances in the all-anti form, in which models show that one set of H8 atoms appears to be significantly closer to nearby phosphates than the other. In the all-syn form, models show the H8 atoms all appear to be in more similar environments, which may explain the failure to observe more than one set of resonances at the field strength we used. Presumably, these large octamolecular complexes would most easily form by gradual association and readjustment of four of the self-intercalated bimolecular structures.

A slow equilibrium would exist among these five different complexes at high concentrations of **1**, with K^+ highly favoring the two octamolecular complexes. Because the smaller, less easily dehydrated Li^+ is less able to stabilize quartets, the resulting mixture has approximately similar amounts of the bimolecular, the two tetramolecular, and the two octamolecular complexes. Although Li^+ does not normally stabilize quartet structures, in this case the presence of two aligned guanines in one molecule presents unique circumstances. c-GMP−IMP (**2**) is unable to form any of these quartet structures because the lack of one amino prevents the full quartet hydrogen bonding. The tethered c-di-GMP (**3a**, and presumably **3b**) are restricted in their abilities to form quartet structures with K^+. An equilibrium among these five structures for c-di-GMP in a bacterial cell might provide a range of options for the actions of this signaling molecule that would significantly depend on its own concentration as well as local K^+ concentrations, or the concentrations of other as yet unidentified effectors. The subcellular compartmentalization and gradients that are known to affect the signaling ability of c-di-GMP[12] may be taking advantage of the equilibrium we describe here. As first proposed by Wang,[23] the tetramolecular complexes may participate in biological pathways by intercalating aromatic groups between the two quartets. We further speculate that the octamolecular complexes may serve as a way to sequester c-di-GMP in an inactive state, with the bimolecular complex providing the active form for signaling. Additional work in our laboratory is underway to further characterize the structural details of these five different complexes, as well as explore in more depth the equilibrium among them.

Conclusion

We have demonstrated that c-di-GMP, an important bacterial signaling molecule involved in biofilm formation and other pathogenic processes, can adopt a mixture of five different but related structures in ratios that are sensitive to both its concentration and the metal present. A bimolecular self-intercalated structure is dominant at dilute concentrations with Li^+, Na^+, Cs^+, and Mg^{2+}, while it is accompanied by one or more quartet complexes with K^+, Rb^+, and NH_4^+. At higher concentrations with K^+ the bimolecular structures associate and rearrange primarily to two stable octamolecular self-intercalated quartet complexes, one all-syn and one all-anti. Two minor tetramolecular quartet complexes are also present, one all-syn and one all-anti. At the higher concentrations with Li^+ the tetramolecular and octamolecular quartet complexes (each with syn and anti versions) are present in approximately equal amounts, along with the bimolecular structure.

Acknowledgment. This work was supported by a grant from NIH (EB002809). We thank Kenneth J. Breslauer, James Elliott, and Jens Völker in this department for assistance with the CD and helpful discussions.

Supporting Information Available: Synthesis of **2**, **3a**, and **3b**; first derivative curves of UV melting profiles; full UV spectra of **1** in Li^+, Na^+, K^+, Rb^+, NH_4^+, and Mg^{2+}; translational diffusion rates for **1** with K^+ and Li^+; 1D NMR of **1**, **2**, **3a**, and **3b**. This material is available free of charge via the Internet at http://pubs.acs.org.

JA0613714